Biomacromolecules

ARTICLE

pubs.acs.org/Biomac

Poly(2-hydroxyethyl methacrylate) for Enzyme Immobilization: Impact on Activity and Stability of Horseradish Peroxidase

Sarah M. Lane,[†] Zhifeng Kuang,[†] Jeannie Yom,[†] Shafi Arifuzzaman,[‡] Jan Genzer,[‡] Barry Farmer,[†] Rajesh Naik,[†] and Richard A. Vaia*[,†]

[†]Air Force Research Laboratory, Materials and Manufactoring Directorate, Wright-Patterson AFB, Ohio 45433-7750, United States

[‡]Department of Chemical & Biomolecular Engineering, North Carolina State University, Raleigh, North Carolina 27695-7905, United States

Supporting Information

ABSTRACT: On the basis of their versatile structure and chemistry as well as tunable mechanical properties, polymer brushes are well-suited as supports for enzyme immobilization. However, a robust surface design is hindered by an inadequate understanding of the impact on activity from the coupling motif and enzyme distribution within the brush. Herein, horseradish peroxidase C (HRP C, 44 kDa), chosen as a model enzyme, was immobilized covalently through its lysine residues on a *N*-hydroxysuccinimidyl carbonate-activated poly(2-hydroxyethyl methacrylate) (PHEMA) brush grafted chemically onto a flat impenetrable surface. Up to a monolayer coverage of HRP C is achieved, where most of the HRP C resides at or near the brush−air interface. Molecular modeling shows that lysines 232 and 241 are the most probable binding sites, leading to an orientation of the immobilized HRP C that does not block the active pocket of the enzyme. Michaelis−Menten kinetics of the immobilized HRP C indicated little change in the K_m (Michaelis constant) but a large decrease in the V_{max} (maximum substrate conversion rate) and a correspondingly large decrease in the k_{cat} (overall catalytic rate). This indicates a loss in the percentage of active enzymes. Given the relatively ideal geometry of the HRPC-PHEMA brush, the loss of activity is most likely due to structural changes in the enzyme arising from either secondary constraints imposed by the connectivity of the *N*-hydroxysuccinimidyl carbonate linking moiety or nonspecific interactions between HRP C and DSC-PHEMA. Therefore, a general enzyme−brush coupling motif must optimize reactive group density to balance binding with neutrality of surroundings.

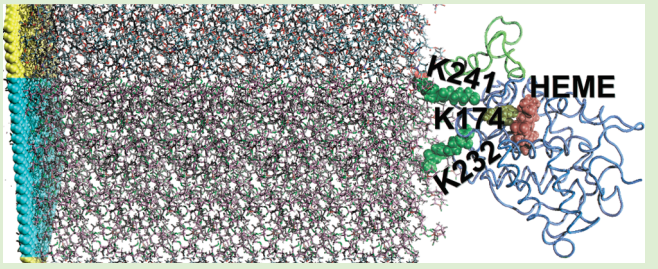

INTRODUCTION

Enzymes provide nature the ability to perform complex reactions with high specificity. For this reason, enzymes are used in many industrial applications, where they enable targeted rate enhancement of critical reactions and biotransformations. Additionally, the specificity of enzymes constitutes the basis of numerous sensing devices. For example, glucose oxidase is often used in devices to measure blood glucose levels.[1] In many applications, immobilization of the enzyme on or within a support is important for ease of enzyme reclamation and reuse as well as enhancement of the enzymatic stability and activity.[2−4] Simple anchoring or imbedding of the enzyme, however, does not always lead to enhanced enzymatic properties. The impact of immobilization on the enzyme depends on many factors, including the enzyme itself, the physical and chemical characteristics of the support, the location of the enzyme on or within the support, or the method of immobilization.[5,6] Although substantial research has been devoted to determining the relative importance of these immobilization factors, many different, and sometimes conflicting, accounts of how particular enzymes are affected by immobilization abound.[6−8]

Polymer brushes provide an excellent platform to establish a robust understanding of the immobilized environment because numerous features of the brush architecture and thus the local environment of the enzyme can be controlled exquisitely. A polymer brush comprises layer of polymer chains that are attached via covalent or strong multidentate secondary interactions to a surface at a high areal density such that the chains are forced to adopt an extended, stretched conformation.[9,10] Two of the most common methods of making polymer brushes include "grafting from" and "grafting to" methodologies. A "grafting from" polymer brush is fabricated by first chemically grafting a polymerization initiator to a surface and then growing the brush from the initiator centers using polymerization techniques, such as atom transfer radical polymerization (ATRP) or ring-opening metathesis polymerization.[10] In the "grafting to" method, the polymer is synthesized ex situ and then immobilized on the surface with any number of means such as covalent or electrostatic

Received: February 7, 2011
Revised: March 21, 2011
Published: March 25, 2011

interactions.[10] Both routes have their advantages and disadvantages depending on the application. See refs 9 and 10 for a detailed discussion of the various grafting methods.

Overall, the nanoscale dimensionality (1−50 nm), swellability, and relative softness of polymer brushes are commensurate to protein assemblies. Numerous research teams are beginning to exploit these attributes as platforms for the adhesion of cells and proteins.[11−16] These initial studies demonstrated retention of enzyme activity upon immobilization and that increasing brush thickness afforded more enzyme immobilization.[11−13] However, with thicker brushes, a fraction of the enzymes was located within the brush, which slowed down diffusion of the substrate, resulting in a lower relative activity. Goplan et al. demonstrated with near-edge X-ray absorption fine structure (NEXAFS) spectroscopy that ribonuclease A (RNase A, 14kD) was randomly oriented when immobilized on poly(acrylic acid) brushes, which indicated that a single residue was not favored for RNase binding.[12] In another study, they determined the Michaelis constant (K_m) of RNase immobilized on poly(2-vinyl-4,4-dimethyl azlactone) brushes.[13] In these studies, the small increase in K_m of the immobilized RNase was attributed to partial blockage of the active site, arising from a random orientation caused by multiple residues capable of coupling.

In this work, we provide further insight into how the activity of enzymes is affected by immobilization on a polymer brush and correlate activity with the orientation and possible structural changes of the bound enzyme using experimental and computational results. Indeed, relating well-defined Michaelis−Menten kinetic values to the properties of the system can provide key understanding to how the different aspects of immobilization, such as structural changes, orientation, and microenvironment, affect enzyme activity. We chose to use a "grafted-from" poly(2-hydroxyethyl methacrylate) (PHEMA) polymer brush[17,18] and horseradish peroxidase C (HRP C) as the model enzyme. PHEMA is approved by the FDA for use in certain medical devices and resists protein fouling.[17] We have shown in previous papers that PHEMA can be functionalized readily with *N*,*N*′-disuccinimidyl carbonate (DSC) rendering it reactive toward primary amines.[19] HRP C is an enzyme that is hardy, abundant, highly active, and well-characterized.[20] In the presence of hydrogen peroxide, HRP C will catalyze the oxidation of numerous substrates from nonchromogenic to chromogenic providing a facile method for quantifying its activity.[20] In this Article, we correlate Michaelis−Menten kinetics and stability of HRP C immobilized on DSC-activated PHEMA with experimental and computational modeling results. HRP C resides mostly at the air−brush interface, and the active pocket is oriented away from the brush and thus unhindered. However, a decrease in activity is seen, which we attribute to noncovalent, nonspecific interactions between the activated brush and HRP C, which results most likely in structural changes and inactivation of a large percentage of the immobilized enzyme.

EXPERIMENTAL SECTION

Reagents. Horseradish peroxidase Type XI was purchased through Sigma Aldrich. As reported by Sigma Aldrich, HRP Type XI is composed primarily of the isozyme HRP C. The substrate, 2,2′-azino-bis-(3-ethylbenzthiazoline-6-sulfonic acid) (ABTS), was purchased as 10 mg tablets from Sigma Aldrich. The initiator, [11-(2-bromo-2-methyl) propionyloxy]-undecyl trichlorosilane (BMPUS), was synthesized according to the literature.[21] The copper(I) chloride, purchased through Sigma Aldrich, was further purified by stirring three times in glacial acetic acid for 15 min, stirring three times in ethanol for 15 min, and finally stirring twice in diethyl ether for 15 min. Unless specified otherwise, all other reagents were purchased from Sigma Aldrich and used as received.

Instrumentation. A 2 Amp Sonicor (SC-101TH), with an operating frequency of ∼50 kHz was used for rinsing. UV−vis spectroscopy (Cary 5000 equipped with an internal designed stirring temperature-controlled sample holder) was performed to monitor substrate conversion. Dry polymer brush thicknesses were determined with a variable angle ellipsometer (Senetech SE400) using a wavelength of 632.8 nm, with angles ranging from 40 to 70°, and using the accompanying software for fitting Ψ and Δ curves from the multiangle data. A bulk refractive index of 1.512 for PHEMA was assumed.[22] Note that for film thicknesses below 20 nm, refractive index differences in the range anticipated for the post functionalization ($\Delta n \approx 0.1$) resulted in an insignificant change in the calculated thickness (±10%). Reported average thicknesses and error were determined from three different measurements on the same sample and three different samples.

Elemental compositions and coupling efficiencies were determined using X-ray photoelectron spectroscopy (XPS) (Surface Instruments) M-probe instrument operated at a base pressure of 3×10^{-7} Pa using an operating voltage of 10 kV and a spot size of 800 μm^2. To obtain the depth profiles, the samples were sputtered at 2 s intervals, with a 500 mV Ar^+ ion beam. ESCA 2000 software was used to interpret the XPS data.

Polymer Brush Preparation. PHEMA brushes were prepared by "grafting from" polymerization based on ATRP on account of its ability to form polymers with low polydispersity and high grafting density. Silicon wafers (Wafer World) were cut into smaller pieces, generally 1.2 cm by 8 cm, and exposed to ultraviolet radiation/ozone (UVO) treatment (Novascan, PSDP) for 10 min. This treatment generates a large concentration of surface-bound hydroxyl groups required for the attachment of the polymerization initiator. The ATRP initiator, BMPUS, was attached to the silicon surface by immersing the UVO-treated wafer in the initiator solution (50 μL of 5% BMPUS toluene solution in 20 mL anhydrous toluene) at −10 °C for 18 h. To decrease the grafting density of the PHEMA brush, we can replace a fraction of the BMPUS on the surface by *N*-decyltrichlorosilane with the addition of this molecule to the BMPUS initiator solution. The BMPUS-coated wafers were then sonicated twice for 10 min in 20 mL of toluene to remove unreacted species. ATRP polymerization of HEMA[23] was carried out in methanol/water using a mixture containing 37.45 g of HEMA, 25.5 g of methanol, 7 mL of water, 2.33 g of bipyridine, 0.663 g of CuCl, and 0.05 g of $CuCl_2$. The polymerization time was adjusted to range between 2 and 5 h to achieve a desired brush thickness of ∼15 nm. After polymerization, the wafers were sonicated twice for 10 min in 20 mL of methanol. The XPS showed no residual copper and good agreement between the theoretical and experimental elemental percentages.

The polymer brush growth was done in accord with published reports by the Genzer group.[24] For these conditions (BMPUS initiator layer deposited with very similar conditions), the molecular weight, *M*, of methacrylates and acrylates by size exclusion chromatography (Genzer et al. determined), combined with polymer thickness, provided an estimate for the chain grafting density as ∼0.45 chains/nm^2.[25] On the basis of this, ∼0.4 chains/nm^2 was considered to be reasonable estimate for this study. For the samples with reduced grafting density, the intensity of the Br 3d peak of the initiator coated wafers was analyzed with XPS. Using the surface density of the undiluted chains (∼0.4 chains/nm^2) and assuming that the Br peak intensity is directly proportional to the surface density of the initiator, the following equation was used to calculate the surface density of the diluted initiator

$$\frac{\sigma_{\text{diluted}}}{0.4\ \text{chains/nm}^2} = \frac{\text{Br peak}_{\text{diluted}}}{\text{Br peak}_{\text{undiluted}}}$$

Whereas the grafting density of the brush may be less than that of the

initiator, we found that the percent decrease in dry brush thickness determined using ellipsometry corresponded fairly well with the percent decrease in Br peak intensity.

DSC-PHEMA. To ensure that the measured results were not impacted by variations of chain density or chain length on different wafers, experiments were performed on a single brush wafer that was fractured into 0.5 cm by 1.2 cm pieces. The silicon wafers coated with PHEMA brushes were first sonicated in 5 mL of methylene chloride and then immersed in a deoxygenated solution of 0.1 M *N,N′*-disuccinimidyl carbonate and 0.1 M 4-dimethylaminopyridine in anhydrous *N,N*-dimethylformamide (DMF) for 24 h at room temperature.[19] The specimens were then rinsed thoroughly with DMF and methylene chloride.

HRPC-PHEMA. Onto the polished side of the DSC-PHEMA coated wafer was spotted a solution of 1 mg/mL (unless specified otherwise) HRP C dissolved in pH 7, 5 mM phosphate buffer. This was allowed to sit for 2 h at 4 °C and was then rinsed with 2 mL of pH 7, 5 mM phosphate buffer. The wafer was then placed in 1.5 mL of pH 7, 5 mM phosphate buffer for 12 h at 4 °C to allow desorption of any physisorbed enzyme. For the rinsings with different stringencies, Rinse 1 was performed with gentle manual rocking of the wafer in 1.5 mL of pH 7, 5 mM phosphate buffer for 2 min, followed by placement of the wafer in 1.5 mL of pH 7, 5 mM phosphate buffer for 12 h at 4 °C. Rinse 2 was performed with gentle manual rocking of the wafer in 1.5 mL of pH 7, 25 mM phosphate buffer for 2 min, followed by placement of the wafer in 1.5 mL of pH 7, 5 mM phosphate buffer for 12 h at 4 °C. Rinse 3 was performed with gentle manual rocking of the wafer in 1.5 mL of pH 7, 25 mM phosphate buffer with 0.01% Tween 20 for 2 min, followed by placement of the wafer in 1.5 mL of pH 7, 5 mM phosphate buffer for 12 h at 4 °C.

Activity. To determine the activity of the HRPC-PHEMA brush and free HRP C in solution, we freshly prepared a 3 mL solution consisting of 0.4−8.0 mM ABTS and 0.1% H_2O_2 in pH 5, 50 mM citrate-phosphate buffer. For free HRP C in solution, 10 μL of freshly prepared 2.7×10^{-7} M HRP C in pH 7, 5 mM phosphate buffer was added to the previous solution. The solution was then mixed thoroughly and placed quickly in the UV−vis spectrometer for analysis. For HRPC-PHEMA, the HRPC-PHEMA wafer was taken out of the storage buffer, rinsed twice with 1 mL of buffer, and suspended in the ABTS/H_2O_2 solution. Subsequently, the sample was placed in the UV−vis spectrometer for analysis. The immobilized sample was stirred vigorously during analysis. For all samples, the absorbance was measured at 415 nm for 2 min at a 0.1 s interval. In data analysis, only the initial linear portion of the absorbance was considered. To determine K_m and V_{max}, we fit the substrate concentration (S) and initial rate (V_0) data to the well-known Michaelis−Menten algorithm ($V_0 = V_{max}S/(K_m + S)$) by means of OriginPro 8.0 SR4.

Stability. To determine the stability of free HRP C in solution, samples of free HRP C were prepared with a 2.4×10^{-8} M concentration in the desired buffer solution. These samples were stored at 4 °C from 1 to 4 days. After sitting for the set period of time, 10 μL of this solution was added to a freshly prepared 3 mL solution of 0.86 mM ABTS and 0.1% H_2O_2 in pH 5, 50 mM citrate buffer. The solution was mixed thoroughly and then placed promptly in the UV−vis spectrometer. To determine the stability of the immobilized HRP C, a similar experiment was performed, where HRP C was immobilized on the polymer brush, rinsed twice with 1 mL of 5 mM, pH 7 phosphate buffer and then placed in 1 mL of the desired buffer. The samples were stored at 4 °C from 1 to 4 days. After sitting for a set period of time, the sample activity was analyzed by UV−vis by suspending in 3 mL of freshly prepared 0.86 mM ABTS and 0.1% H_2O_2 in pH 5, 50 mM citrate buffer. These samples were stirred vigorously during analysis. For all samples, the absorbance was measured at 415 nm for 2 min at a 0.1 s interval. In data analysis, only the initial linear portion of the absorbance was considered. For the experiments that examined the effect of temperature, freshly prepared free HRP C (10 μL of 2.7×10^{-7} M HRP C) or HRPC-PHEMA was placed in a cuvette with 2.9 mL of 50 mM, pH 5 citrate buffer and allowed to sit for 2 min at a desired temperature before the addition of ABTS and H_2O_2 to make 3 mL total of 0.86 mM and 0.1%, respectively. The samples were mixed well, and the absorbance was measured at 415 nm for 2 min at a 0.1 s interval. In data analysis, only the initial linear portion of the absorbance was considered.

Docking Method. A four-mer DSC-PHEMA acted as a ligand. Lamarckian genetic algorithm implemented in AutoDock3.05[26] was used to predict the most possible association poses with each lysine residue in HRP C. The AutoDock program was performed around each lysine independently using default parameters. Fifty initial conformations of the 4-mer polymer were randomly generated. From the 50 individuals in the first generation, no more than 2.7×10^4 generations were produced using the Lamarckian genetic algorithm. Each generation had 50 individuals, including one survival from the last generation. The global and local energy evaluations were performed. The docking process terminated when a maximum 2.5×10^6 energy evaluations was reached. The conformation with the lowest binding energy was selected. The above process was repeated 100 times so that 100 conformations were retained.

Molecular Dynamics Simulations. All simulation systems were created using tleap utility in Amber. When necessary, chloride ions were added to neutralize the system. The TIP3P water model was used in all simulations with a margin 0.8 nm to solute. Periodic boundary conditions were used in all three dimensions. PME method was used to calculate the long-range electrostatic forces. All systems were first minimized for 2000 steps, then heated to 300 K, and finally equilibrated until the desired quantity converged under NVT configurations.

RESULTS

Immobilizaiton of HRP C. To correlate changes in activity of immobilized HRP C with its orientation on and binding mechanism to the DSC-PHEMA brush, it is necessary to start with a controlled, well-characterized system. As previously shown, DSC reacts with the hydroxyl groups of PHEMA to form an *N*-hydroxysuccinimidyl (NHS) carbonate moiety.[19] The NHS carbonate reacts with primary amines, such as those found on the lysine residues of HRP C, covalently immobilizing the species on the brush (Figure 1). Table 1 summarizes the elemental analysis (obtained by XPS) of the PHEMA surface before activation, after DSC activation and after HRP C immobilization on the DSC-PHEMA. Table 1 also shows nonactivated PHEMA surfaces with different grafting densities after exposure to 1 mg/mL HRP C solution.

At high PHEMA grafting densities (~0.4 PHEMA chains/nm^2), no detectable nonspecific adsorption of HRP C on nonactivated PHEMA is seen, as demonstrated by the lack of N1s peak in XPS, which would arise solely from the protein. The grafting density of the brush can be decreased by including an alkyl-trichlorosilane along with the BMPUS in the initiator solution to reduce the initiator concentration on the surface. The reduced grafting densities were calculated from the decrease in the Br 3d5 signal in XPS of the diluted BMPUS initiator. Note that the dry brush thicknesses made with 100% BMPUS initiator were ~15 nm, as measured with ellipsometry. The lower grafting-density brushes had smaller thicknesses corresponding to the decreased initiator density. The resistance to nonspecific adsorption was seen at grafting densities as low as ~0.08 PHEMA chains/nm^2. At these grafting densities, the surface is covered uniformly with extended swollen PHEMA chains and is consistent with prior reports of the nonfouling nature of PHEMA.[27] A lower grafting density

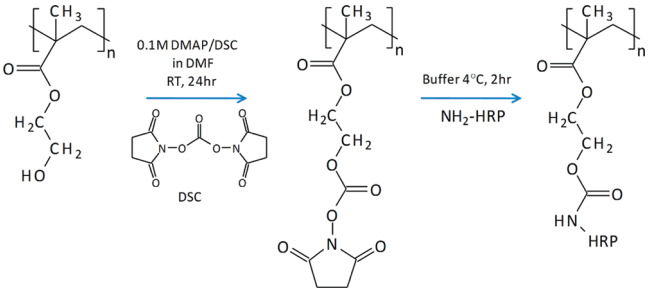

Figure 1. Scheme showing the brush modification steps.

Table 1. XPS Elemental Analysis of PHEMA Brushes (a) Nonspecific Absorption of 1 mg/mL HRP C on Nonactivated PHEMA, (b) DSC Activated of 0.4PHEMA (DSC-PHEMA), and (c) Stability of HRP C Bound to DSC-PHEMA to Increasing Stringency of Rinses (Rinses 1−3 in the Experimental Section)

sample	% C1s (ideal)	% O1s (ideal)	% N1s (ideal)
[a] 0.4PHEMA/nm^2	67.9 (66.7)	32.1(33.3)	0 (0)
0.08PHEMA/nm^2	67.6	32.4	0
0.004PHEMA/nm^2	62.4	32.3	5.3
[a] DSC-PHEMA	64.0 (57.9)	31.4(37.0)	4.0 (5.3)
[b] HRPC-DSCPHEMA-Rinse1	65.2 (62.0)	27.3(25.5)	7.5(12.5)
HRPC-DSCPHEMA-Rinse2	65.0	27.1	7.8
HRPC-DSCPHEMA-Rinse3	65.2	27.3	7.6

[a] Ideal elemental percentage comes from the empirical formula for PHEMA and DSC-PHEMA, respectively. [b] Ideal elemental percentage, which assumes a perfect close packed monolayer of HRP C completely attenuating the signal from the brush, comes from the empirical formula for HRP C.

(~0.004 PHEMA chains/nm^2), however, resulted in nonspecific adsorption. This is most likely due to an increased interaction between HRP C and the hydrophobic decytrichlorosilane used to dilute the initiator sites. At these low grafting densities, the swollen chains can adopt a more coiled configuration, exposing a greater amount of the underlying surface to the protein.

As previously shown, intermediate graft densities, albeit nonfouling, enable small (14 kDa) enzyme incorporation and a reduction in overall activity due to the gradient in accessibility of the substrate to the enzyme.[11,23] Thus, focusing on the highest grafting density brush (i.e., 0.4 PHEMA chains/nm^2), Table 1 summarizes the excellent agreement between XPS and idealized surface compositions of pure PHEMA, DSC-PHEMA, and a dense monolayer of HRP C, respectively. This agreement confirms the high fidelity and control of the coupling chemistry. Furthermore, the insensitivity of surface chemistry (no significant change in the N1s intensity) to washes with increasing stringency, where Rinse 1 is the least stringent and Rinse 3 is the most (see the Experimental Section), confirms the robust covalent bonding of HRP C to the DSC-PHEMA brush (Table 1c).

Crucial to quantifying the activity of the immobilized enzyme is to determine the areal density of proteins on the surface and their distribution within the brush. Doing so on a 2D surface at monolayer concentrations without resorting to radioisotopes is, however, not trivial because of the low absolute number of proteins. A number of methods were examined, such as using the Coomassie blue dye, XPS, and ellipsometry; the latter being the most reliable.

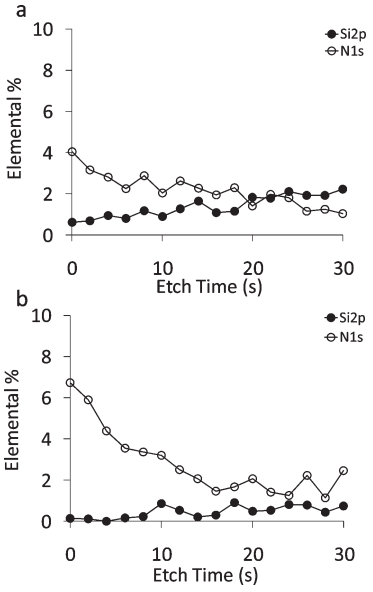

Figure 2. Depth profile of the (a) DSC-PHEMA and (b) HRPC-PHEMA using sputtering and XPS.

In our system, Coomassie blue appeared to bind to more than just the HRP C, giving an unrealistically high value. Quantitative XPS intensity difference between the N1s peak of HRPC-PHEMA and the Si 2p peak of the substrate was troublesome because of the redeposition of sputtered material and the difficulty of distinguishing the N 1s signal from the DSC and HRP C. However, surface XPS analysis of the DSC-PHEMA indicates 75% activation at the surface (three of four monomers). Increase in the N 1s signal after treating the DSC-PHEMA with HRP C is evidence of HRP C coupling. Qualitative distribution of DSC and HRP C through the brush could be inferred from XPS sputtering profiles for Si2p and N1s peaks (Figure 2) because it is reasonable to assume for sputtering conditions that more material is being sputtered away than redeposited. This assessment is reinforced by the steady but slight increase in the Si peak, which shows that the mass on the surface is being slowly removed. Therefore, the qualitative trends reflect the top half of the brush. The peak area of the N1s, before sputtering and after each cycle of 2 s of mild sputtering, drops off considerably for HRPC-PHEMA, whereas that of the DSC-PHEMA is more gradual. This indicates that the HRP C is sequestered toward the air−brush interface, whereas the DSC activation is somewhat more distributed through the brush, as would be expected for the much smaller *N,N′*-disuccinimidyl carbonate molecule. Also, note that the Si2p peak increases only slightly during sputtering, demonstrating that at least half of the brush remains at 30 s sputtering time (~50−60% of a 15 nm brush based on the attenuation of the Si2p peak using the standard uniform overlayer model).[28]

Ellipsometry provided the most reliable method for determining the thickness of an enzyme layer. Because XPS confirmed that the vast majority of enzyme is at the brush surface, the ellipsometric change in the dry DSC-PHEMA brush thickness before and after HRP C immobilization can thus be converted to the number or areal density of protein on the surface.[15] The surface coverage of the enzyme is then

$$\sigma = \rho h_d \qquad (2)$$

where σ is the surface density of HRP C (g/cm^2), ρ is the

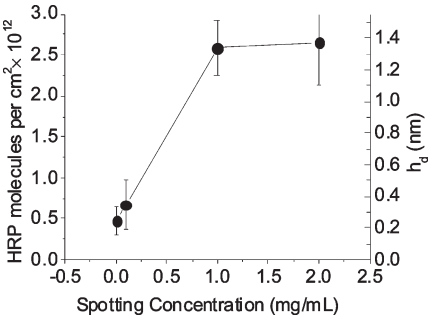

Figure 3. Surface coverage achieved with different HRP C spotting concentrations at 2 h determined using height changes with ellipsometry.

Table 2. Results of the Fits for the Michaelis–Menten Kinetics Experiments for Free HRP C in solution and HRP C Immobilized on the DSC-PHEMA Brush

sample	K_m (mM)	V_{max} (mM/sec)	k_{cat} (sec^{-1})
HRP solution	1.45 ± 0.57	7.8 ± 0.56 × 10^{-4}	1010
HRP immob.	1.51 ± 0.44	7.9 ± 1.8 × 10^{-6}	9.8

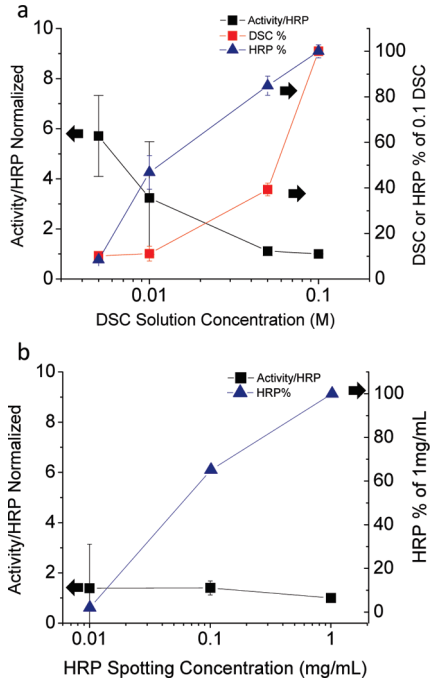

Figure 4. (a) Comparison of the activity/HRP C immobilized on DSC-PHEMA with decreased surface DSC activation (taken as a percentage of the 0.1 M DSC activation solution). The amount of HRP C immobilized decreased at a slower rate than the DSC functionalization. (b) Comparison of the activity/HRP C with decreasing HRP C surface concentration (taken as a percentage of the 1.0 mg/mL HRP C sample). The decreased HRP C surface concentrations were achieved by decreasing the concentration of HRP C in the spotting solution.

approximate density of HRP C based on proteins of similar MW (1.41 g/cm^3),[29] and h_d is the height change due to the immobilization of HRP C. Figure 3 shows the surface coverage of HRP C determined from ellipsometry with increasing concentrations of the HRP C spotting solution. A maximum HRP C coverage of 2.6 × 10^{12} molecules/cm^2 was observed at ~1 mg/mL. Assuming monolayer coverage, this corresponds to a center-to-center enzyme spacing of 6 nm. Considering that the dimensions of recombinant HRP C are 3.7 nm × 3.7 nm × 5.2 nm, the estimated surface coverage is almost a monolayer and is consistent with the surface XPS elemental percentages of the unsputtered HRPC-PHEMA (Table 1). Furthermore, AFM of the dry brush before and after HRP C immobilization (Supporting Information) showed little change in the topological features, indicating that the enzyme is depositing as a uniform layer and is not composed of multienzyme aggregates. The mean-squared roughness decreases slightly from 2.4 nm for DSC-PHEMA to 1.5 nm for the HRPC-PHEMA, which may indicate that HRP C prefers to reside in the concave regions of the brush's topological features to maximize the interactions between the brush and enzyme. Note that HRP C extracted from the horseradish root contains ~18–22 wt % of flexible carbohydrate chains attached to eight surface asparagines. The additional carbohydrate chains and associated water molecules will increase the effective size of HRP C, which is consistent with observations, and the supposition that a monolayer is formed at ~2.6 × 10^{12} molecules/cm^2.

Activity. The rate of substrate conversion by the immobilized enzyme relative to free enzyme provides a general assessment of the impact of immobilization. It is difficult, however, to ascertain the mechanistic origin for an enhanced or reduced rate from these studies alone, which necessitates the determination of the Michaelis–Menten kinetics. For a simple single-substrate enzyme, the initial rate of substrate conversion is measured over a wide range of substrate concentrations. A fit of the initial rates to the Michaelis–Menten equation provides the maximum rate (V_{max}) and the Michaelis constant (K_m), which is the substrate concentration at one-half of V_{max}. V_{max} is dependent on the enzyme concentration, and thus the value k_{cat}, which is V_{max} divided by the enzyme concentration, also provides a meaningful measure of activity comparison. Table 2 lists the K_m, V_{max}, and k_{cat} for free HRP C and PHEMA-immobilized HRP C, which were obtained using the standard procedure where the initial rate of substrate conversion was measured at different substrate concentrations; then, the data were fitted to the equation given in the Experimental Section. Note that the activity measurements of free HRP C and immobilized HRP C were made with approximately the same total moles of enzyme so that their K_m and V_{max} values can be directly compared. Ultimately, the bulk concentrations in the assay solution were similar; however, it is important to keep in mind that the local concentration of the enzyme on DSC-PHEMA was higher than that of the enzyme in solution. The K_m was similar for both the free and immobilized HRP C (1.45 ± 0.57 versus 1.51 ± 0.44 mM, respectively). In contrast, the V_{max} of the immobilized HRP C was two orders of magnitude lower than the free HRP C (7.9 ± 1.8 × 10^{-6} mM/sec versus 7.8 ± 0.56 × 10^{-4} mM/sec, respectively). Therefore, the overall catalytic rate, k_{cat}, which is calculated by dividing V_{max} by the concentration of HRP C, is also two orders of magnitude lower for the immobilized HRP C compared with the free enzyme (8.6 versus 987 s^{-1}).

DSC Concentration. To test whether excess DSC activation could play a role in the loss of the activity of HRP C, we decreased the amount of DSC on the surface while monitoring the initial rate of substrate oxidation by HRP C immobilized on the surface. Both the DSC and HRP C functionalizations were determined using XPS. As shown in Figure 4a, decreasing the DSC solution concentration in the brush activation step resulted in a rapid

decrease in the extent of DSC surface activation. However, the amount of HRP C immobilized on the surface did not decrease commensurately. For example, a decrease in the DSC activation by ~60% resulted in only a ~20% decrease in the amount of HRP C immobilized, indicating excess DSC activation compared with the HRP C footprint at the higher DSC concentrations. However, at the lowest DSC surface concentration, the amount of immobilized HRP C dropped off substantially. A decrease in DSC surface functionalization by 10- to 20-fold provided a reduction in immobilized HRP C by 2- to 10-fold. The activity per HRP C went up at the lower DSC concentrations, indicating that excess DSC may play a role in the decreasing activity of the immobilized HRP C. In contrast, decreasing the amount of HRP C immobilized on the surface, while keeping the DSC concentration constant, did not appear to affect the activity per enzyme molecule (Figure 4b).

Stability. Enzyme immobilization or encapsulation is oftentimes used to increase the storage lifetime or the stability of the enzyme in organic solvents at elevated temperatures or, in general, under conditions that normally lead to protein deactivation.[30] Local rigidity imparted by the encapsulant or the immobilizing linkage is believed to help preserve the enzyme tertiary structure.[3] The initial rate of oxidation of ABTS, V_0, by HRP C and HRPC-PHEMA was taken as a simple measure of how activity was affected over the course of 3 days under three buffer conditions (Figure 5). Over this period, all systems showed some loss of activity, but as expected, the HRPC-PHEMA had either the same stability or better stability than the free HRP C in solution, especially in the pH 7, 5 mM phosphate buffer, where the percent retained activity of HRPC-PHEMA is three times greater than free HRP C in solution.

Figure 6 summarizes the impact of temperature on free HRP C and HRPC-PHEMA by comparing the initial rate of oxidation of ABTS by the enzyme. The highest initial rate was observed at 50 °C for HRPC-PHEMA and 40 °C for free HRP C. The maximum initial rate at ~40−50 °C is reportedly due to changes in the tertiary structure of the heme pocket at this temperature.[31] The decrease in activity at 60 °C is likely due to the beginning stages of the melting of the secondary structure.[31] Although slight differences are seen, the temperature profiles for the initial rate of the HRPC-PHEMA and free HRP C are very similar, and any difference cannot be discerned beyond the experimental error. This indicates that binding does not substantially increase thermal stability of the tertiary structure and that the increased stability to buffers reflects restricted access to degradation sites.

Molecular Modeling. Computational modeling provides a refined view of the binding mechanism, and orientation of HRP C on the DSC-PHEMA. HRP C is a monomeric glycoprotein (44 kDa) with 308 residues including six lysines and the N-terminus blocked by pyroglutamate.[20] As noted above, there are eight glycosylation sites, Asn 13, 57, 158, 186, 198, 214, 255, and 268, with the total carbohydrate by weight of HRP C being 18−22%, depending on the source. The crystal structure of HRP C without the carbohydrate (Figure 7) has been solved at 2.15 Å resolution (PDB code 1ATJ) and is shown in Figure 7.[32]

The most accessible lysines were initially determined with AutoDock3.0.5 by randomly generating 2.5×10^6 conformations of a 4-mer DSC-PHEMA segment near each lysine. AutoDock program produced 100 most probable binding poses between

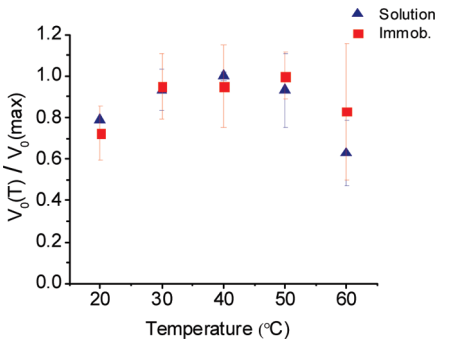

Figure 6. Temperature stability of free (triangles) and immobilized HRP C (squares) as reflected in the relative change in the initial rate V_0 with respect to the maximum initial rate.

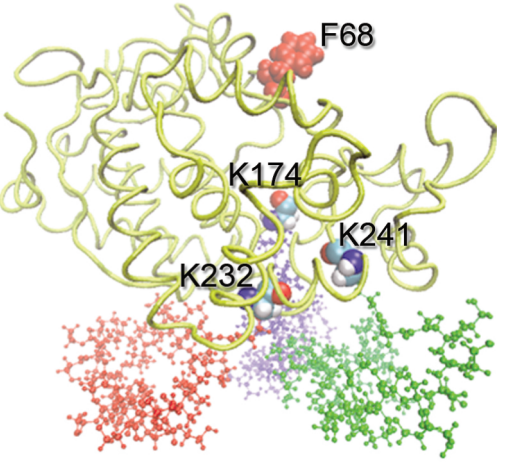

Figure 7. Crystal structure of HRP C with three 20-mers of DSC-PHEMA interacting with Lys 232, 174, and 241 and the residue Phe-68 guarding the active pocket of HR.

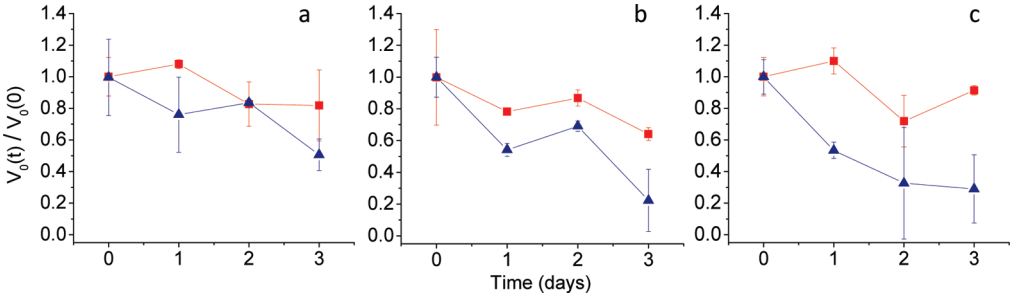

Figure 5. Stability of free (triangles) and immobilized HRP C (squares) as reflected by relative change in initial oxidation rate of ABTS $V_0(0)$ with time, *t*. (a) pH 6, 5 mM phosphate buffer; (b) pH 7, 50 mM phosphate buffer; and (c) pH 7, 5 mM phosphate buffer. All samples were stored at 4 °C.

Table 3. Minimum Distance ($-d(N_\varepsilon,C)$: −nm) between N_ε Atom of Lysine Residues and the Carbonate Carbon of DSC-PHEMA for Each Docked 4-mer DSC-PHEMA and the Interaction Energy ΔE (kcal/mol) between HRP C and the DSC-PHEMA Conformation Attaining the Minimum Distance

lysine	65	84	149	174	232	241
ΔE	−63.11	−72.88	−68.51	−46	−64.67	−47.27
$d(N_\varepsilon,C)$	0.71	0.75	0.44	0.48	0.34	0.47

HRP C and DSC-PHEMA. The minimum distance between the carbonate carbon of DSC-PHEMA polymer chain and the epsilon nitrogen of lysine was measured and tabulated in Table 3. The interaction energy between HRP C and the DSC-PHEMA conformation attaining the minimum distance was calculated and shown in Table 3 for all six lysines. Lys 65 and Lys 84 are significantly farther than the vdW separation distance needed for covalent interactions. In addition, Lys 149 is engaged in a salt bridge with Asp 258, leaving Lys 174, 232, and 241 as possible attachment points. The DSC-PHEMA can approach much closer to Lys 232 with a lower energy than the other two residues, making it a more favorable candidate.

To investigate further the energetic possibilities and determine if there was a preference to single or multiple binding of the residues Lys 241, 232, and 174, we investigated seven comparable systems by modifying the lysines one by one using three polymers, each having 20 monomers (Figure 7). On one end of each polymer, two of the PHEMA monomers were DSC-modified. The seven possible binding combinations involving one, two, or all three lysines 232, 241, and 174 were investigated. Three systems showed the lowest and approximately equal energies within the experimental error. These were single binding to the brush through Lys 241 or 232 or biresidue binding using both Lys 241 and 232. Therefore, in addition to single binding through Lys 232 as the AutoDock calculations show, single binding through Lys 241 or multiple binding through Lys 241 and 232 are also likely possibilities. Single or multiple binding through Lys 174 resulted in higher energies for the system, indicating that these events are less likely.

DISCUSSION

The activity of a simple single-substrate enzyme reflects four process steps: substrate diffusion to the active pocket, substrate binding, substrate-to-product conversion, and finally release of the product. Immobilization can alter activity by impacting any of these processes through structural changes in the enzyme, such as denaturation; blocking the active site; inhibiting diffusion of the substrate to the enzyme; or general microenvironment effects.[6] Michaelis−Menten kinetics provides a direct assessment of these processes and yields a more accurate picture of immobilization than comparing the turnover number of a substrate at a single substrate and enzyme concentration. The Michaelis constant (K_m) in many cases is equal to the dissociation constant (K_D) of the enzyme−substrate complex; therefore, the reciprocal of K_m is interpreted as a direct measure of the enzyme substrate affinity. The maximum velocity (V_{max}) is the rate of substrate conversion when the enzyme is saturated with the substrate. k_{cat} reflects the rate-limiting process at the enzyme active site. For horseradish peroxidase, the catalytic cycle involves a $2e^-$ oxidation of the enzyme by hydrogen peroxide.[33] The oxidized enzyme then reverts to the resting state enzyme via two successive $1e^-$ reactions with reducing substrate molecules.

So far, there is only one other report of Michaelis−Menten kinetics of an enzyme on a polymer brush, where Goplan et al. studied RNase, a ∼13.7 kDa protein, immobilized on poly-(2-vinyl-4,4-dimethyl azlactone).[13] The K_m for the bound RNase was higher than the free RNase by a factor of 1.9. On the basis of similarities in the activity profiles at different pH values and temperatures of bound and free RNase, Goplan et al. concluded that the difference in K_m for the bound and free enzyme was due to blocking of the active site of the enzyme and not caused by structural changes in the active pocket. The general azlactone coupling, which binds RNase through any of its hydroxyl- or primary amine-containing residues, resulted in a random orientation of the protein. This statistical distribution of orientation challenges the determination of how binding through specific residues would affect activity.

The more specific DSC coupling to primary amines and finite lysine residues on HRP C improves the ability to decouple variations in orientation on the brush with structural changes within the protein. Note that HRP C naturally has its N-terminus blocked by a pyroglutamyl group so that it is unable to react.[34] In addition, not all six lysine residues are accessible because of protein structure folding. A number of researchers have looked at the modification of HRP C with a variety of relatively small synthetic groups to determine experimentally the accessibility of the ε-amino groups of the six lysine residues in HRP C. O'Brien et al. demonstrated through various methods including proteolytic fragmentation and peptide sequencing that modification of HRP C with ethylene-glycolbis(*N*-hydroxysuccinimidylsuccinate) (EGNHS) resulted in complete modification of Lys 232; partial modification of Lys 174 and 241; and very little reaction of Lys 65, Lys 68, and Lys 149.[34] These are all consistent with the computational prediction that Lys 232 and 241 are the most probable binding points.

A separate study by Mogharrab et al. investigated modifying HRP C lysines with anthroquinone.[35] Experimentally, Mogharrab and coworkers observed a small increase in activity, reported as a slightly lower K_m and a modest increase in the V_{max}. MD simulations by Mogharrab revealed that the binding of anthraquinone to Lys 174, 232, and 241 slightly modified the structure of HRP C in such a way to open up some of the residues near the active site, facilitating the access of hydrogen peroxide and substrate to the heme pocket. Nevertheless, given that the accessible lysines are not integral in the function of the active pocket, modification with small molecules did not dramatically change the structure or activity, as Mogharrab observed. Indeed, surrounding the bottleneck of the active site are hydrophobic residues (Phe 68, Phe 142, and Phe 179, Figure 7) that shuttle in and out the hydrogen peroxide and the substrate. These are on the opposite side of HRP C as Lys 232 and Lys 241. Therefore, on the basis of the prior reports, modeling discussion herein, and location of Lys 232 and Lys 241, the similarity in the K_m values between free and immobilized HRP C indicates that immobilization on the DSC-PHEMA does not block the active pocket.

Indeed, partially blocking the active site of the enzyme or simply immobilizing an enzyme onto or into a surface can cause diffusion limitations, also known as mass transfer limitations. To reduce the effect of diffusion, it is advantageous that the enzyme is located at the surface of the brush. In addition, vigorous stirring was employed during the kinetics assay. It has been previously shown that diffusion-limited immobilized enzymes result in a higher K_m, whereas V_{max} (achievable at much higher substrate concentrations) would ultimately be unaffected.[36,37] Surface−charge effects of the

support have also been shown to change the K_m but not V_{max}.[36,37] This is exactly the opposite of what is seen here, making it unlikely that diffusion limitations are the cause of the low V_{max} and k_{cat}.

Because V_{max} depends on the enzyme concentration whereas K_m does not, a decrease in V_{max} while K_m remains the same, as observed here, indicates the effective enzyme concentration has decreased by complete inactivation of some percentage of the enzyme. The most likely cause of the decrease in active enzyme concentration is a structural change caused by nonspecific interactions of the enzyme with the brush. As shown in Figure 4, decreasing the amount of DSC on the surface results in an approximately five-fold increase in the activity of the immobilized enzyme compared with higher DSC concentrations. Even though HRP C does not nonspecifically bind to unmodified PHEMA, the DSC-PHEMA is highly functionalized, and this surface may be more amenable for nonspecific interactions with HRP C in addition to lysine binding. The structural changes HRP C undergoes with the nonspecific interactions must be dramatic enough to cause loss of activity for a large percentage of the enzymes. However, a small but reproducible percentage of immobilized HRP C appears to retain activity and thus the structure. This is supported by the temperature−activity profile in Figure 6. Although it is not clear why all enzymes do not lose their activity, perhaps the ones that do retain their structure represent those that initially bind to the DSC-PHEMA with multiple lysines. An increase in the stability of the structure of an enzyme with increasing immobilization points is certainly well-supported by the literature.[3]

Of the reports of HRP C immobilization on a solid support, only a handful of these examples report the Michaelis−Menten kinetics of the system.[7,8,38] For example, Vianello et al. used a succinylated, amino-silane self-assembled monolayer (SAM)-modified glass surface to prepare carboxylic acid terminated surface.[7] They then activated the carboxylic acid moieties with 1-ethyl-3-(3-dimethylaminopropyl)carbodiimide and *N*-hydroxysuccinimide, followed by HRP C binding. The results of their Michaelis−Menten kinetics study showed a decrease in the K_m by a factor of ~2 and a decrease in the V_{max} and k_{cat} by a factor of ~50. These values are similar to those reported herein. However, the authors did not provide a reason for the decrease in V_{max}, but because they use similar chemistry to immobilize HRP C, the cause of the decrease in activity could be similar to that of the PHEMA system.

Others have reported examples where similar immobilization strategies did not result in a dramatic decrease in activity. For example, Devi et al. looked at the immobilization of HRP C on micrometer-sized beads of acrylamide-2-hydroxyethyl methacrylate copolymer using activation of both amino and hydroxyl groups with glutaraldehyde and *p*-benzoquinone, respectively, allowing covalent coupling of the enzyme through its lysines with both monomers.[38] This polymer is swellable, and HRP C is most likely immobilized not only on the surface but also within the beads. HRP C immobilized through this method showed a slight increase in V_{max} and a similar K_m compared with free HRP C in solution. Devi's study is consistent with a trend seen in the literature where immobilization involving encapsulation of HRP C within a material, rather than immobilizing directly at the solvent-support interface, results in greater activity retention, possibly because of 3D support of the enzyme structure by the encapsulant material,[38−40] whereas HRP C immobilized at the solvent−support interface would undergo more structural changes to maximize attractive nonspecific interactions to the 2D surface.

CONCLUSIONS

Using HRP C as a model enzyme and PHEMA as a model support, we investigated how immobilizing an enzyme on a densely functionalized brush impacts activity and stability. Covalent immobilization is achieved by highly functionalizing the surface with DSC giving a dense monolayer of HRP C that resides close to the surface of the brush. Michaelis−Menten kinetics show that the K_m of free HRP C and HRPC-PHEMA is fairly similar, whereas the V_{max} and k_{cat} have decreased by almost two orders of magnitude. This indicates a loss of the effective enzyme concentration and that a large percentage of the enzyme is deactivated. Modeling shows that the HRP C is most likely binding through Lys 232 or Lys 241, which would not cause blocking of the active pocket. Decreasing the DSC surface activation results in an increase in activity per HRP C molecule. Therefore, the loss of activity is likely due to structural changes resulting from nonspecific interactions between the enzyme and the DSC activated brush. A small percentage of enzymes retain their activity, which may indicate that these bind using multiple lysines or other residues, as demonstrated through the simulations. These results indicate the need to balance covalent immobilization while maintaining a passive surrounding.

ASSOCIATED CONTENT

Supporting Information. Michaelis−Menten data and AFM images. This material is available free of charge via the Internet at http://pubs.acs.org.

REFERENCES

(1) Wilson, R.; Turner, A. P. F. *Biosens. Bioelectron.* **1992**, *7*, 165.
(2) Dulay, M. T.; Baca, Q. J.; Zare, R. N. *Anal. Chem.* **2005**, *77*, 4604.
(3) Mateo, C.; Palomo, J. M.; Fernandez-Lorente, G.; Guisan, J. M.; Fernandez-Lafuente, R. *Enzyme Microb. Technol.* **2007**, *40*, 1451.
(4) Luckarift, H. R.; Spain, J. C.; Naik, R. R.; Stone, M. O. *Nat. Biotechnol.* **2004**, *22*, 211.
(5) Cao, L.; Langeny, L. v.; Sheldon, R. A. *Curr. Opin. Biotechnol.* **2003**, *14*, 387.
(6) Cao, L. *Carrier Bound Immobilized Enzymes*; Wiley-VCH: Weinheim, Germany, 2005.
(7) Vianello, F.; Zennaro, L.; Paolo, M. L. D.; Rigo, A.; Malacarne, C.; Scarpa, M. *Biotechnol. Bioeng.* **2000**, *68*, 488.
(8) Tiller, J. C.; Rieseler, R.; Berlin, P.; Klemm, D. *Biomacromolecules* **2002**, *3*, 1021.
(9) *Polymer Brushes: Synthesis, Characterization, Applications*; Brittain, B., Advincula, R., Rühe, J., Caster, K., Eds.; Wiley-VCH: Weinheim, Germany, 2004.
(10) Zhao, B.; Brittain, W. J. *Prog. Polym. Sci.* **2000**, *25*, 677.
(11) Xu, F. J.; Cai, Q. J.; Li, Y. L.; Kang, E. T.; Neoh, K. G. *Biomacromolecules* **2005**, *6*, 1012.
(12) Cullen, S. P.; Liu, X.; Mandel, I. C.; Himpsel, F. J.; Gopalan, P. *Langmuir* **2008**, *24*, 913.
(13) Cullen, S. P.; Mandel, I. C.; Gopalan, P. *Langmuir* **2008**, *24*, 13701.
(14) de las Heras Alarcón, C.; Farhan, T.; Osborne, V. L.; Huck, W. T. S.; Alexander, C. *J. Mater. Chem.* **2005**, *15*, 2089.
(15) Harris, B. P.; Kutty, J. K.; Fritz, E. W.; Webb, C. K.; Burg, K. J. L.; Metters, A. T. *Langmuir* **2006**, *22*, 4467.
(16) Hatakeyamaa, H.; Kikuchia, A.; Yamatoa, M.; Okanoa, T. *Biomaterials* **2007**, *28*, 3632.
(17) Bhat, R. R.; Tomlinson, M. R.; Genzer, J. *J. Polym. Sci., Part B* **2005**, *43*, 3384.
(18) Peluso, G.; Petillo, O.; Anderson, J. M.; Ambrosio, L.; Nicolais, L.; Melone, M. A. B.; Eschbach, F. O.; Huang, S. J. *J. Biomed. Mater. Res.* **1997**, *34*, 327.

(19) Diamanti, S.; Arifuzzaman, S.; Elsen, A.; Genzer, J.; Vaia, R. *Polymer* **2008**, *49*, 3770.
(20) Veitch, N. C. *Phytochemistry* **2004**, *65*, 249.
(21) Matyjaszewski, K.; Miller, P. J.; Shukla, N.; Immaraporn, B.; Gelman, A.; Luokala, B. B.; Siclovan, T. M.; Kickelbick, G.; Vallant, T.; Hoffmann, H.; Pakula, T. *Macromolecules* **1999**, *32*, 8716.
(22) Maggio, R. D.; Rossi, F.; Fambri, L.; Fontana, A. *J. Non-Cryst. Solids* **2004**, *345*−*346*, 591.
(23) Tomlinson, M. R.; Genzer, J. *Langmuir* **2005**, *21*, 11552.
(24) Tomlinson, M. R.; Genzer, J. *Polymer* **2008**, *49*, 4837.
(25) Wu, T.; Gong, P.; Szleifer, I.; Vlček, P.; Šÿubr, V.; Genzer, J. *Macromolecules* **2007**, *40*, 8756.
(26) Morris, G. M.; Goodsell, D. S.; Halliday, R. S.; Huey, R.; Hart, W. E.; Belew, R. K.; Olson, A. J. *J. Comput. Chem.* **1998**, *19*, 1639.
(27) Mei, Y.; Elliott, J. T.; Smith, J. R.; Langenbach, K. J.; Wu, T.; Xu, C.; Beers, K. L.; Amis, E. J.; Henderson, L. *J. Biomed. Mater. Res., Part A* **2006**, *79*, 974.
(28) Popat, K. C.; Sharma, S.; Desai, T. A. *J. Phys. Chem. B* **2004**, *108*, 5185.
(29) Fischer, H.; Polikarpov, I.; Craievich, A. F. *Protein Sci.* **2004**, *13*, 2825.
(30) Schoemaker, H. E.; Mink, D.; Wubbolts, M. G. *Science* **2003**, *299*, 1694.
(31) Chattopadhyay, K.; Mazumdar, S. *Biochemistry* **2000**, *39*, 263.
(32) Gajhede, M.; Schuller, D. J.; Henriksen, A.; Smith, A. T.; Poulos, T. L. *Nat. Struct. Mol. Biol.* **1997**, *4*, 1032.
(33) Rodriguez-Lopez, J. N.; Smith, A. T.; Thorneley, R. N. F. *J. Biol. Chem.* **1996**, *271*, 4023.
(34) O'Brien, A. M.; Ó'Fágáin, C.; Nielsen, P. F.; Welinder, K. G. *Biotechnol. Bioeng.* **2001**, *76*, 278.
(35) Mogharrab, N.; Ghourchian, H.; Amininasab, M. *Biophys. J.* **2007**, *92*, 1192.
(36) Rosevear, A.; Kennedy, J. F.; Cabral, J. M. S. *Immobilized Enzymes and Cells*; Adam Hilger: Bristol, England, 1997.
(37) Shiraishi, F. *J. Ferment. Bioeng.* **1995**, *79*, 373.
(38) Shukla, S. P.; Devi, S. *Process Biochem.* **2005**, *40*, 147.
(39) Takahashi, H.; Li, B.; Sasaki, T.; Miyazaki, C.; Kajino, T.; Inagaki, S. *Chem. Mater.* **2000**, *12*, 3301.
(40) Naik, R. R.; Tomczak, M. M.; Luckarift, H. R.; Spain, J. C.; Stone, M. O. *Chem. Commun.* **2004**, 1684.